# Anomalous X-ray Scattering Study of the Quasi-crystalline $Al_{65}Cu_{20}Fe_{15}$ Alloy

E. Matsubara and Y. Waseda

Research Institute of Mineral Dressing and Metallurgy (SENKEN), Tohoku University, Sendai 980, Japan

A. P. Tsai, A. Inoue, and T. Masumoto

Institute for Materials Research, Tohoku University, Sendai 980, Japan

Z. Naturforsch. **45a**, 50–54 (1990); received October 10, 1989

The environmental radial distribution functions (RDFs) around Cu and Fe as well as the ordinary RDF of an as-quenched $Al_{65}Cu_{20}Fe_{15}$ alloy have been determined by anomalous x-ray scattering (AXS) and conventional x-ray diffraction techniques. The experimental information indicates that a strong directional dependence along the symmetrical axes exists for the Cu atoms but not for the Fe atoms. Almost identical RDFs were also obtained in both the as-quenched and fully-annealed states of the $Al_{65}Cu_{20}Fe_{15}$ alloy. Thus, the small differences observed between diffraction profiles of the as-quenched and annealed samples of this alloy may be attributed to defects or strains introduced during the rapid quenching process.

## Introduction

Since the discovery of icosahedral symmetry in rapidly-quenched Al-Mn alloys by Shechtman et al. [1], many other binary and ternary alloys forming the icosahedral phase have been found. However, the icosahedral phases in these alloys except Al-Li-Cu are formed as metastable phases and usually contain many defects, phason strains and dislocations, which obscure their fundamental structural features.

Recently, Tsai et al. [2] found a rather new thermodynamically stable icosahedral phase of Al-Cu-Fe alloys, x-ray and electron diffraction, and high-resolution electron microscopy [3] of which revealed a high degree of structural perfection. Thus, this quasi-crystalline alloy appears to be one of the most appropriate systems to investigate the structural details.

In the present study, we applied the anomalous x-ray scattering (hereafter referred to as AXS) to the quasi-crystalline $Al_{65}Cu_{20}Fe_{15}$ alloy at the Cu and Fe K-absorption edges in order to determine the environmental structure around Cu and Fe atoms. There is a slight difference between the x-ray diffraction profiles of the as-quenched and annealed states of this alloy [2]. Therefore both alloys were also studied by ordinary x-ray diffraction.

Reprint requests to Dr. E. Matsubara, Research Institute of Mineral Dressing and Metallurgy, Tohoku University, Sendai 980/Japan.

## Experimental

An ingot of $Al_{65}Cu_{20}Fe_{15}$ was prepared by arc-melting from mixtures of pure aluminum (99.99 wt%), copper (99.99 wt%) and iron (99.9 wt%). From the master ingot, ribbons of about 0.02 mm thickness and 1 mm width were prepared by a single-roller melt-spinning technique. An annealed sample was obtained by annealing the as-quenched ribbons for 172.8 ks (48 hrs) at 1023 K (0.90 $T_m$) and for 172.8 ks at 1073 K (0.94 $T_m$) in vacuum, where $T_m$ is the melting temperature of the alloy (1141 K) [2]. For the x-ray measurements, powder samples were prepared by grinding these as-quenched and annealed ribbons.

The AXS measurements were carried out with synchrotron radiation at the Photon Factory of the National Laboratory for High Energy Physics, Tsukuba, Japan. Since the details of the experimental setting and analysis are explained in [4], only some additionals required in the present work are given below. The AXS intensities were observed at 25 and 300 eV below the Cu and Fe K-absorption edges. Since the so-called EXAFS (extended x-ray absorption fine structure) and XANES (x-ray absorption near edge structure) phenomena appearing on the high energy side of the edge make the anomalous dispersion terms complicated, and since extremely intense fluorescent radiation causes trouble in the scattering measurements, only the low energy side was used in the present AXS mea-

0932-0784 / 90 / 0100-0050 $ 01.30/0. – Please order a reprint rather than making your own copy.

surements. Even on the lower energy side of the edge, however, weak K $\alpha$ and K $\beta$ fluorescent radiations, mainly arising from the tail of the band pass of the monochromator crystal, were observed during the measurement at 25 eV below the edge. Although the K $\alpha$ radiation was experimentally eliminated by measuring with a solid state detector, the energy of the K $\beta$ radiation is too close to separate it from the elastic scattering. Thus, this K $\beta$ radiation was theoretically estimated from the K $\alpha$ radiation and the ratio of K $\beta$ to K $\alpha$ [5], and was corrected in a similar way in the previous works [4, 6].

A monochromatic incident beam at any energy from 4 to 20 keV can be obtained with a silicon 111 double-crystal monochromator, its optimum energy resolution being about 7 eV at 10 keV. Since the incident beam intensity decays with time in a synchrotron radiation source, it was monitored with a nitrogen-gas-flow type ion-chamber placed in front of the sample. In the analysis, all of the observed intensities were converted to intensities per photon by using these monitor counts [7]. A non-negligible intensity of the higher harmonics diffracted by the Si 333 plane was observed in the present measurements. Thus, by intentionally detuning the second Si crystal of the double crystal monochromator, the intensity of the higher harmonics was reduced to less than 0.5%, although about 20% of the first order diffracted intensity was lost.

## Data Processing

Only the fundamental equations are given below, while the details of the analysis may be found, e.g. in [4] and [8].

On the low energy side of the edge of a specific element A, the detected variation in intensity is attributed only to the change of the real part of the anomalous dispersion term $f'$ of A. Thus, the difference between the scattering intensities measured at two energies $E_1$ and $E_2$ ($E_1 < E_2$) is given by

$$\begin{aligned}\Delta I_A(Q) &= I(Q,E_1) - I(Q,E_2)\\ &= c_A(f'_A(E_1) - f'_A(E_2))\\ &\cdot \int_0^{Q_{max}} 4\pi r^2 \sum_{j=1}^{N} \mathrm{Re}\,[f_j(Q,E_1) + f_j(Q,E_2)]\\ &\cdot (\varrho_{Aj}(r) - \varrho_{0j}) \frac{\sin(Qr)}{Qr}\,\mathrm{d}r, \end{aligned} \tag{1}$$

where

$$I(Q,E_j) = I_{eu}^{coh}(Q) - \langle f^2\rangle \tag{2}$$

and

$$\langle f^2\rangle = \sum_{j=1}^{N} c_j f_j^2. \tag{3}$$

$Q$ is the wave vector, and $c_j$ and $f_j$ are the atomic fraction and the x-ray atomic scattering factor of the $j$th element, respectively. $Q_{max}$ is the maximum value of $Q$ used for the measurement. $N$ is the number of constituent elements in a sample, $\varrho_{Aj}(r)$ the number density function of the $j$th atom around the element A, and $\varrho_{0j}$ the average number density for the $j$th element. "Re" indicates the real part of the function in the braces. For the x-ray atomic scattering factors, the values tabulated in the International Tables for X-ray Crystallography, Vol. IV [9] were used, and for the anomalous dispersion terms the theoretical values [8] computed by Cromer and Liberman's method [10] were used.

The environmental radial distribution function (RDF) for A, which represents the radial distribution of atoms around an A atom, was determined by the Fourier transform of the quantity $Q\,\Delta I_A(Q)$:

$$\begin{aligned}4\pi r^2 \varrho_A(r) &= 4\pi r^2 \varrho_0\\ &+ \frac{2r}{\pi} \int_0^{Q_{max}} \frac{Q\,\Delta I_A(Q)\sin(Qr)}{c_A(f'_A(E_1) - f'_A(E_2))\,W(Q)}\,\mathrm{d}Q, \end{aligned} \tag{4}$$

and

$$W(Q) = \sum_{j=1}^{N} c_j (f_j(Q,E_1) + f_j(Q,E_2)), \tag{5}$$

where $\varrho_A(r)$ is the number density function around A and $\varrho_0$ the average number density. This energy-derivative method with the AXS based upon the idea of Hosoya [11] and Shevchik [12] was first used by Fuoss et al. [13] with synchrotron radiation in 1981 under the name of differential anomalous scattering (DAS), although the principle of the anomalous x-ray scattering itself is unchanged.

On the other hand, the scattering intensities measured with the Mo K $\alpha$ radiation were also used to estimate the ordinary RDF which represents the average structure of a sample. The measured intensities are corrected for absorption, polarization and Compton scattering, and converted to absolute units [14]:

$$\begin{aligned}&I_{eu}^{coh}(Q)\\ &= \langle f^2\rangle + \langle f\rangle^2 \int_0^{Q_{max}} 4\pi r^2 (\varrho(r) - \varrho_0) \frac{\sin(Qr)}{Qr}\,\mathrm{d}r, \end{aligned} \tag{6}$$

and

$$\langle f \rangle = \sum_{j=1}^{N} c_j f_j, \tag{7}$$

where $\varrho(r)$ is the average number density function. The Fourier transform of the intensity in (6) gives the ordinary RDF of the system, i.e.

$$4\pi r^2 \varrho(r) = 4\pi r^2 \varrho_0 + \frac{2r}{\pi} \int_0^{Q_{max}} \frac{Q[I_{eu}^{coh}(Q) - \langle f^2 \rangle]}{\langle f \rangle^2} \sin(Qr)\, dQ. \tag{8}$$

By comparing the environmental RDF around A in (4) with the ordinary RDF in (8), the merit of the AXS method is easily recognized. In the present system, for example, the six partial RDFs for the Al-Al, Al-Cu, Al-Fe, Cu-Cu, Cu-Fe and Fe-Fe pairs are overlapped in the ordinary RDF curve. On the other hand, only three partial RDFs of pairs relating to Cu or Fe are included in the environmental RDF around Cu or Fe.

## Results and Discussion

The scattering intensities of the as-quenched $Al_{65}Cu_{20}Fe_{15}$ alloy measured at 6.811 and 7.086 keV below the Fe K-absorption edge, and their difference are shown at the bottom and top of Fig. 1 respectively. The peaks were indexed by the indexing scheme of the icosahedral reflections proposed by Cahn et al. [15]. Following Ishimasa et al. [16], all the indices were multiplied by a factor of 2 to satisfy the parity rule. The numbers in the parentheses at some peaks indicate the directions of the symmetrical axes along which the reflections are located. The differential profile observed by the AXS measurement is essentially similar to the original profiles except for the small difference in relative peak intensity. It implies that the Fe atoms are homogeneously distributed in the alloy. This is consistent with the result obtained by $^{57}Fe$ Mössbauer spectroscopy [17]. The AXS measurements of the as-quenched $Al_{65}Cu_{20}Fe_{15}$ alloy were also carried out at energies of 8.680 and 8.955 keV below the Cu K-absorption edge, and the results are given in Figure 2. Contrary to the results of Fig. 1, regarding the Fe atoms, the differential profile shown at the top of Fig. 2 appears to be significantly different from the original profiles. The differential peak intensities indicate both positive and negative values and vary in each symmetry axis. Thus it may be concluded that the Cu atoms are orderly arranged at particular sites in the icosahedral structure and are not distributed uniformly along every symmetrical direction like Fe.

The environmental RDFs around Fe and Cu are shown in Fig. 3 together with the ordinary RDF calculated from the intensity measured with Mo K $\alpha$ ra-

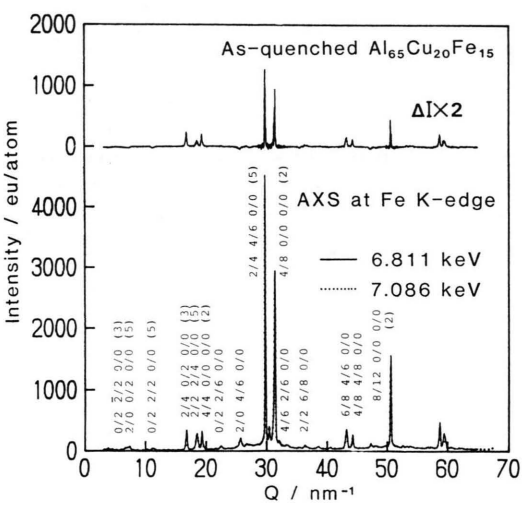


Fig. 1. Differential intensity profile of as-quenched quasi-crystalline $Al_{65}Cu_{20}Fe_{15}$ alloy (top) determined from the intensity profiles (bottom) measured at incident energies of 6.811 and 7.086 keV, which correspond to energies of 25 and 300 eV below the Fe K-absorption edge.

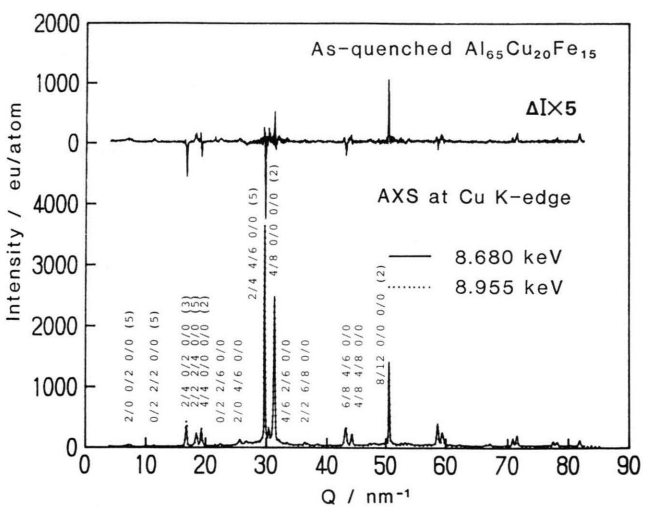


Fig. 2. Differential intensity profile of as-quenched quasi-crystalline $Al_{65}Cu_{20}Fe_{15}$ alloy (top) determined from the intensity profiles (bottom) measured at incident energies of 8.680 and 8.955 keV, which correspond to energies of 25 and 300 eV below the Cu K-absorption edge.

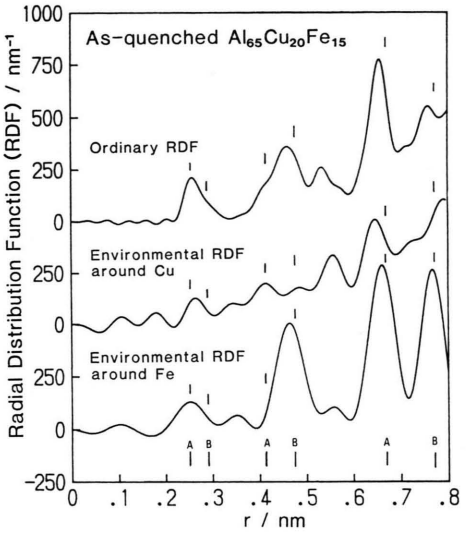


Fig. 3. Ordinary radial distribution function (RDF) and environmental RDFs around Fe and Cu of as-quenched quasi-crystalline $Al_{65}Cu_{20}Fe_{15}$ alloy (density = 4.637 $Mg/m^3$).

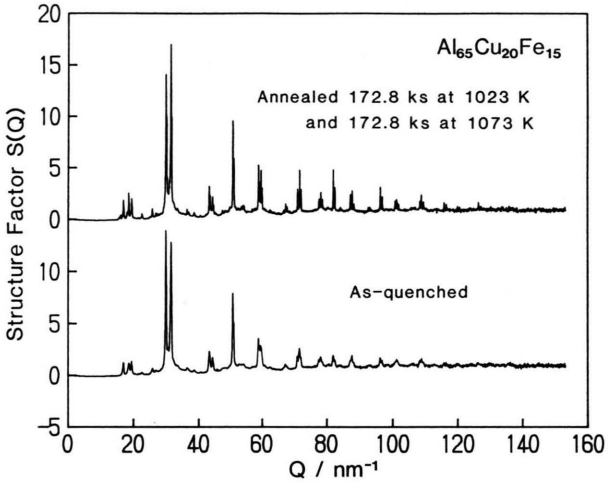


Fig. 4. Structure factors of as-quenched quasi-crystalline $Al_{65}Cu_{20}Fe_{15}$ alloy and the one annealed for 172.8 ks at 1023 K and 172.8 ks for 1073 K.

diation. In the ordinary RDF, the first peak at 0.26 nm has a shoulder at the higher-r side. Such a right-skewed first peak has already been observed in amorphous $Al_{56}Si_{30}Mn_{14}$ and $Al_{77.5}Mn_{22.5}$ alloys [18], and this characteristic structural feature of the first peak was explained by the presence of clusters icosahedrally ordered. On the other hand, both of the first peaks in the environmental RDFs have no shoulder, and their peak maximum coincides with the maximum of the first peak in the ordinary RDF. Furthermore, no clear peak nor shoulder are observed at the position of its shoulder. Taking account of the definition of the environmental RDFs and the concentrations of the constituent elements, the first peak is to be attributed to the correlation of pairs of Al and transition metal and its shoulder to that of Al and Al pairs. A slight difference between the positions of the first peak in both of the environmental RDFs can be qualitatively explained by the different sizes of the Cu and Fe atoms. Coordination numbers and distances calculated from the first peak of the three RDFs are summarized in Table 1. Since the Cu-Al and Fe-Al pairs appear to be located at the maximum of the first peak in the ordinary RDF, the corresponding coordination number was estimated as an average coordination number of Al atoms around Cu and Fe atoms. All of the coordination numbers computed from these three RDFs conform with each other. It is also worth noting that these values are similar to those experimentally

Table 1. Coordination numbers, $N$, and interatomic distances, $r$, for as-quenched quasi-crystalline $Al_{65}Cu_{20}Fe_{15}$ alloy experimentally determined from the first peaks of the ordinary radial distribution function (RDF) and the environmental RDFs around Cu and Fe.

| | $r$/nm | $N$ |
|---|---|---|
| Ordinary RDF | | |
| Al-Cu or Fe | 0.258 | $9.5 \pm 0.2$ (on average) |
| Al-Al | 0.293 | $8.5 \pm 0.3$ |
| Environmental RDF around Cu | | |
| Al-Cu | 0.273 | $8.6 \pm 0.5$ |
| Environmental RDF around Fe | | |
| Al-Fe | 0.253 | $10.8 \pm 0.8$ |

determined in the icosahedral $Al_{73}Mn_{21}Si_6$ alloy by EXAFS measurements at the Al and Mn K-absorption edges [19].

Some positions, which are $n\tau$ times the atomic distances of the first peak maximum and its shoulder, are indicated by arrows A and B in Fig. 3, where $\tau$ is the golden mean and $n$ is integer. Most of the peaks or shoulders in the RDFs are found to be in accord with these positions. This coincidence supports the results by high-resolution electron microscopy that a scaling rule of $\tau$ exists in real space in the Al-Fe-Cu alloy [3, 16]. Consequently, as far as the near-neighboring structure is concerned, the atomic configuration in the icosahedral Al-Cu-Fe alloy is similar to that in the icosahedral Al-Si-Mn alloy. Since the particular concentration of the constituent elements is known to

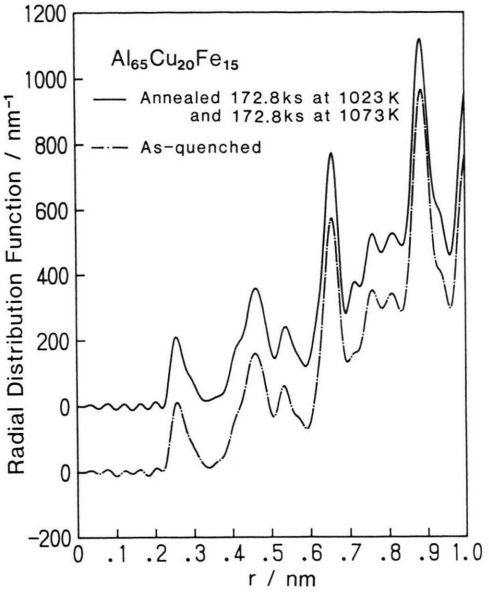


Fig. 5. Ordinary radial distribution functions (RDFs) of as-quenched quasi-crystalline $Al_{65}Cu_{20}Fe_{15}$ alloy and the one annealed for 172.8 ks at 1023 K and 172.8 ks for 1073 K.

form a single icosahedral phase, it is quite reasonable that Cu or Fe atoms occupy particular sites of an icosahedral structure. The present AXS results of Figs. 1 and 2 suggest that the directional dependence along the symmetry axes is strong for Cu atoms but not for Fe atoms. However, the actual message about the particular sites occupied by Cu or Fe atoms in an icosahedral structure of the $Al_{65}Cu_{20}Fe_{15}$ alloy cannot be obtained at the present time.

Structural analyses of the as-quenched and fully annealed states of the $Al_{65}Cu_{20}Fe_{15}$ alloy were carried out by the conventional x-ray diffraction method with Mo K$\alpha$ radiation. The resultant structure factors, $S(Q)=[I_{eu}^{coh}(Q)-\langle f^2\rangle]/\langle f\rangle^2$, are given in Figure 4. As observed by Tsai et al. [2], the essential features of these two diffraction patterns are found to resemble each other, although there are small differences in detail, for example in the region for the three peaks at about 20 nm$^{-1}$ and for the two strong peaks at 30 nm$^{-1}$. The ordinary RDFs calculated from these structure factors using (8) are shown in Figure 5. As seen in these RDFs, the atomic structures are almost identical within a distance of, at least, about 1 nm. Thus, it is not too much to say that the local atomic arrangements of the as-quenched $Al_{65}Cu_{20}Fe_{15}$ alloy are almost unchanged by annealing. Hiraga et al. [3] reported that there exists no phason strain in an Al-Cu-Fe alloy conventionally solidified. Therefore, the small differences recognized in the intensity profiles between the as-quenched and the fully-annealed states of the $Al_{65}Cu_{20}Fe_{15}$ alloy may be attributed to defects, and/or strains introduced during the rapid quenching from the melt.

Part of this research was supported by the Mitsubishi foundation research project on anomalous x-ray scattering of 1986. The authors are grateful to the Ministry of Education, Science and Culture of Japan for a Grant-in-Aid for Scientific Research on Priority Areas (01630001). Part of this research was also supported by the Science Foundation for Light Metals and Alloys. We (EM and YW) want to thank the staff of the Photon Factory, National Laboratory for High Energy Physics, particularly Drs. M. Nomura and A. Koyama for their kind help.

[1] D. Shechtman, I. A. Blech, D. Gratias, and J. W. Cahn, Phys. Rev. Lett. **53,** 1951 (1984).
[2] A. P. Tsai, A. Inoue, and T. Masumoto, Japanese J. Appl. Phys. **26,** L1505 (1987).
[3] K. Hiraga, B. P. Zhang, M. Hirabayashi, A. Inoue, and T. Masumoto, Japanese J. Appl. Phys. **27,** L951 (1988).
[4] E. Matsubara, K. Harada, Y. Waseda, and M. Iwase, Z. Naturforsch. **43a,** 181 (1988).
[5] N. V. Rao, S. B. Reddy, G. Satyanarayana, and D. L. Sastry, Physica **138c,** 215 (1986).
[6] S. Aur, D. Kofalt, Y. Waseda, T. Egami, R. Wang, H. S. Chen, and B. K. Teo, Solid State Commun. **48,** 111 (1983).
[7] E. Matsubara, Y. Waseda, M. Mitera, and T. Masumoto, Trans. Japan. Inst. Met. **29,** 697 (1988).
[8] Y. Waseda, Novel Application of Anomalous X-ray Scattering for Structural Characterization of Disordered Materials, Springer-Verlag, New York 1984, p. 84.
[9] International Tables for X-ray Crystallography, Vol. IV (Kynoch, Birmingham 1974), p. 148.
[10] D. T. Cromer and D. Liberman, J. Chem. Phys. **53,** 1891 (1970).
[11] S. Hosoya, Bull. Phys. Soc. Japan, **25,** 110 (1970).
[12] N. J. Shevchik, Phil. Mag. **35,** 805 (1977).
[13] P. H. Fuoss, P. Eisenberger, W. K. Warburton, and A. Biedenstock, Phys. Rev. Lett. **46,** 1537 (1981).
[14] Y. Waseda, Structure of Non-Crystalline Materials, McGraw-Hill, New York 1980, p. 60.
[15] J. W. Cahn, D. Shechtman, and D. Gratias, J. Mater. Res. **1,** 13 (1986).
[16] T. Ishimasa, Y. Fukano, and M. Tsuchimori, Phil. Mag. Lett. **58,** 157 (1988).
[17] Z. M. Stadnik and G. Stroink, Phys. Rev. B **38,** 10447 (1988).
[18] E. Matsubara, K. Harada, Y. Waseda, H. S. Chen, A. Inoue, and T. Masumoto, J. Mater. Sci. **23,** 753 (1988).
[19] A. Sadoc, A. M. Flank, and P. Lagarde, Phil. Mag. B **57,** 399 (1988).